

CHAPTER 2

MAGNETIC RESONANCE TECHNIQUES

With contributions from Angelika Brückner,
Michel Che Krystyna Dyrek, Daniella Goldfarb,
Piet J. Grobet, Robert A. Schoonheydt and
Bert M. Weckhuysen

Magnetic resonance techniques, and in particular electron spin resonance (ESR), are very powerful and frequently used for probing the oxidation and coordination environment of transition metal ions (TMI) in heterogeneous catalysts. There are a wide variety of ESR techniques available, each with their particular advantages and limitations. CW X-band ESR spectroscopy is the most popular technique because of its availability and possibility to conduct *in situ* measurements, although there is now an increasing use of more advanced techniques, such as ENDOR, ESEEM and high frequency ESR.

All these ESR techniques can be applied at different levels of sophistication: from merely detecting the presence of transition metal ions over the determination of the first coordination sphere around this paramagnetic center up to a detailed description of its electronic structure. Whatever level is being considered, it is important that the user realises both the potential and the limitations of the particular technique. Overinterpretation should certainly be avoided. This holds equally so for underinterpretation, if with some extra effort (*e.g.*, spectrum simulations), more physically meaningful information can be extracted from the experimental data. The systematic and intelligent application of ESR and its related techniques is therefore of paramount importance for a better understanding of the properties of TMI on surfaces in the future.

2.1. General Principles of Magnetic Resonance Techniques

by Bert M. Weckhuysen* and Robert A. Schoonheydt

*Centrum voor Oppervlaktechemie en Katalyse,
Departement Interfasechemie, K.U.Leuven,
Kardinaal Mercierlaan 92, 3001 Leuven, Belgium*

2.1.1. Introduction

Magnetic resonance techniques – often coined as spin resonance spectroscopy – are based on the interaction of a nuclear or electron spin with a magnetic field in the presence of either radio- or microwaves. In the case of nuclear spins, the spectroscopy is called nuclear magnetic resonance (NMR), whereas the detection of electron spins forms the basis of electron spin resonance (ESR) or electron paramagnetic resonance (EPR). ESR has proven to be an excellent technique for studying all paramagnetic oxidation states of transition metal ions (d^n with $n \neq 0$), while NMR is mainly concerned with the study of diamagnetic transition metal ions. An example of the latter is V^{5+} (d^0), which has a nuclear spin I of $7/2$ with a natural abundance of almost 100%. An overview of all the NMR-accessible first-row transition metals and their natural abundance is given in Table II.1.

Table II.1 Overview of the first-row transition metals accessible by NMR.

Element	Sc	Ti	V	Cr	Mn	Fe	Co	Ni	Cu	Zn
Isotope number	45	47	51	53	55	57	59	61	63	67
Nuclear spin	$7/2$	$5/2$	$7/2$	$3/2$	$5/2$	$1/2$	$7/2$	$3/2$	$3/2$	$5/2$
Natural isotopic abundance (%)	100	7.28	99.76	9.55	100	2.19	100	1.19	69.09	4.11

2.1.2. Spin resonance spectroscopy

Most of the vocabulary of spin resonance spectroscopy comes from physics, and we need to be familiar with the fundamental properties of electrons, protons and neutrons before we can understand and utilise the information, which can be

* BMW acknowledges the FWO for a position as postdoctoral research fellow.

extracted from this spectroscopy. A detailed account of spin resonance spectroscopy can be found in numerous textbooks and review papers [1-24].

All elementary particles; *i.e.*, electrons, protons and neutrons, possess the property of a spin. In the macroworld, moving charged bodies generate electric and magnetic fields, and the analogy was adopted in the early 1900s that a spinning electron would do so too. This idea was later extended to protons and neutrons, and the properties of these particles can now also be rationalized by assuming a spinning behavior.

The quantum number associated with the spin property of these elementary particles is equal to $\frac{1}{2}$. The consequence is that all atoms or molecules with unpaired electrons possess a spin. The spin of a nucleus with p protons and n neutrons is entirely dependent on the vectorial sum of the p spins of the protons and the n spins of the neutrons. Therefore only specific isotopes have a non-zero nuclear spin and can be studied by spin resonance spectroscopy (see for example the isotopes of the first-row transition metal ions in Table II.1).

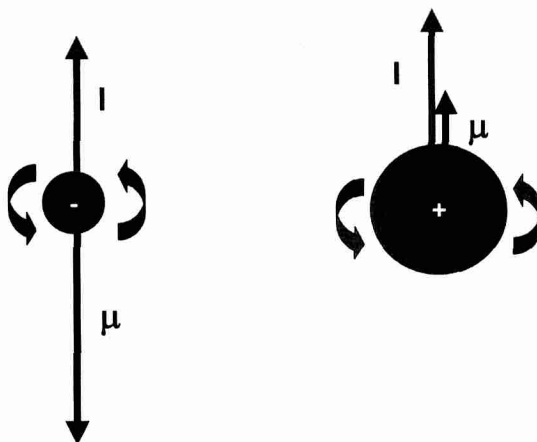


Figure II.1. The spinning electron (left hand side) and the spinning proton (right hand side). Both are shown with the same direction of spin thus their angular momentum vectors point in the same direction, while the vector representing the magnetic moment points in the opposite direction in case of an electron.

An electron and proton can be depicted as a spinning charged body, which is characterized by a spin angular momentum (Figure II.1). This can be represented by an angular momentum vector \vec{I} , obeying the right-hand screw rule for vectors. The module of the vector \vec{I} is – according to quantum mechanics – equal to:

$$|\vec{I}| = \left(\frac{h}{2\pi}\right)\sqrt{I(I+1)} \quad (\text{Eq. II.1})$$

with I , the spin quantum number and h , Planck's constant, which is equal to 6.6×10^{-34} J.s. For protons and electrons – both with $I = \frac{1}{2}$ – the angular momentum vector is equal to $0.87(h/2\pi)$. The quantized values of the spin angular momentum for other spin systems are summarized in Table II.2.

Table II.2 Spin quantum numbers and derived quantities.

Spin quantum number I	Angular momentum I , in units of $h/2\pi$	Number of spin states	Magnetic quantum number m_I – the z-axis components of I
0	0	0	0
$\frac{1}{2}$	0.87	2	$+\frac{1}{2}; -\frac{1}{2}$
1	1.41	3	$+1; 0; -1$
$\frac{3}{2}$	1.94	4	$+\frac{3}{2}; +\frac{1}{2}; -\frac{1}{2}; -\frac{3}{2}$
2	2.45	5	$+2; +1; 0; -1; -2$
$\frac{5}{2}$	2.96	6	$+\frac{5}{2}; +\frac{3}{2}; \frac{1}{2}; -\frac{1}{2}; -\frac{3}{2}; -\frac{5}{2}$

Unlike spinning macroscopic bodies, which can be made to spin in any direction, there are quantised limits to the direction of the angular momentum of elementary particles. These directions are subject to a few simple rules. First, the number of allowed orientations for angular momentum is given by $(2I + 1)$ with I the spin quantum number. Thus, for an electron with $I = \frac{1}{2}$, only two directions are allowed, while for ^{55}Mn with $I = \frac{5}{2}$ six directions are allowed. This is illustrated in Figure II.2. It is important to stress here that the symbol I is usually only used for nuclei, whereas the symbol S is exclusively used for electrons.

Secondly, the allowed values for the magnitude of the momentum can be deduced using magnetic quantum numbers, m_I . The allowed values of spin m_I , are $I, I - 1, \dots, 0, \dots, -(I-1), -I$ (for spin quantum number $I = 1, 2, \dots$) and $I, I - 1, \dots, \frac{1}{2}, -\frac{1}{2}, \dots, -I$ (for spin quantum number $I = \frac{1}{2}, \frac{3}{2}, \frac{5}{2}, \dots$). Table II.2 shows the number of orientations (often named spin states) for common cases and the allowed values ($1, \frac{1}{2}, -\frac{1}{2}$, and so on) usually refer to the values of 'spin'. In order to measure \vec{I} we have to supply a magnetic field B_0 with which \vec{I} can directly interact. No experiment can be performed that will measure the whole spin angular momentum \vec{I} of a spin, and we have to define the direction of the applied field as lying along the z-axis of a set of rectangular cartesian coordinate system (Figure II.2). Only those orientations of \vec{I} , which have components along the z-axis (\vec{I}_z), are experimentally observed. The angle θ between \vec{I} and \vec{I}_z can be calculated from $\cos\theta = 0.5/0.87 = 0.57$, and thus $\theta = 55^\circ$. It is important to stress that the angular momentum vector \vec{I} is oriented randomly with respect to the x- and y-axes, and thus we can construct two cones, each of half angle 55° . The angular momentum vectors can lie anywhere on the surface of these cones (Figure II.2).

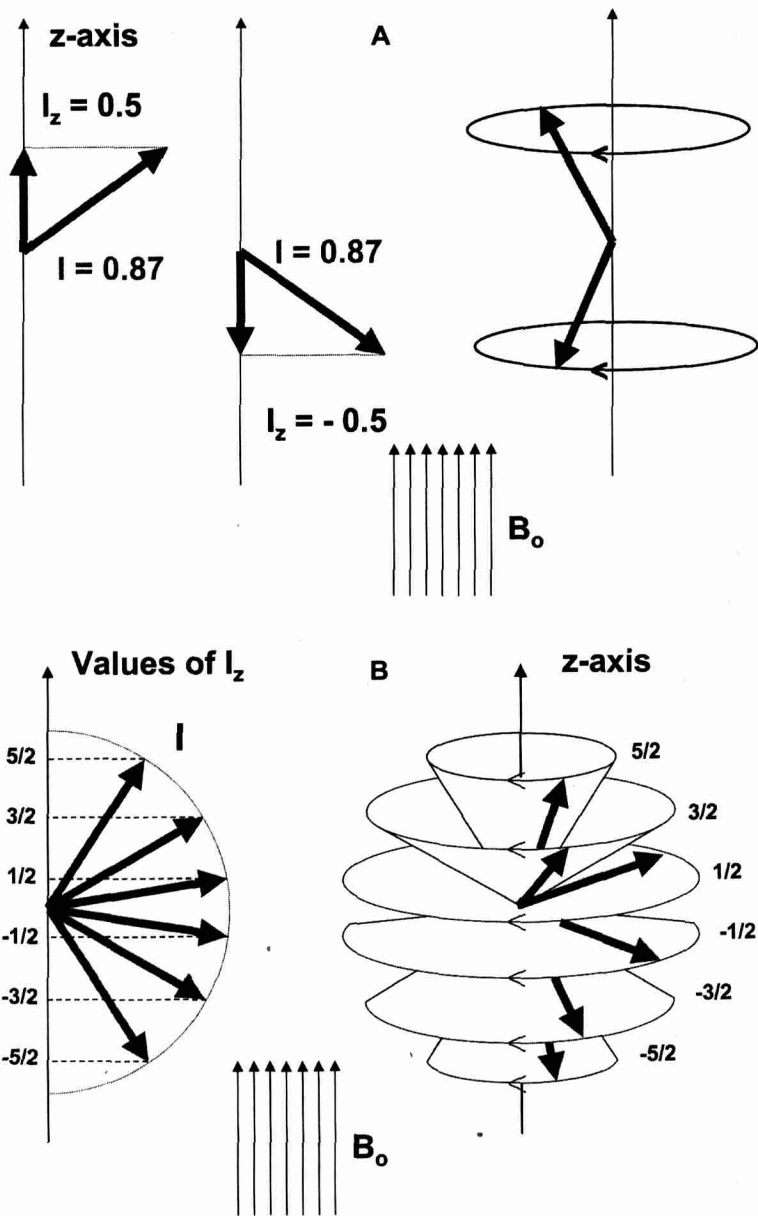


Figure II.2. (A) The allowed directions of the spin angular momentum for $I = 1/2$. The component along the z -axis can only take two values, and the angle between \vec{I} and I_z can be calculated from its cosine; and (B) The allowed directions of the spin angular momentum for $I = 5/2$. The cones of precession are also included (right hand side figure).

Table II.3. The gyromagnetic ratio γ and the ESR/NMR frequency for resonance of a free electron and the first-row transition metals.

Isotope	Gyromagnetic ratio γ ($\times 10^7$) [rad.T ⁻¹ .s ⁻¹]	ESR/NMR frequency [MHz] ¹
Free electron	-18218.78	65856.57
⁴⁵ Sc	6.5081	24.328
⁴⁷ Ti	-1.5105	5.646
⁵¹ V	7.0453	26.336
⁵³ Cr	-1.512	5.651
⁵⁵ Mn	6.608	24.70
⁵⁷ Fe	0.8661	3.238
⁵⁹ Co	6.317	23.61
⁶¹ Ni	-2.394	8.949
⁶³ Cu	7.0974	26.530
⁶⁷ Zn	1.6768	6.2679

¹ Resonance frequency for a magnetic field B = 2.35 T = 23500 Gauss.

In the absence of a magnetic field, the spin may be regarded as spinning randomly. When an external magnetic field B_0 is supplied to the system, the spins must adopt one of the orientations, as determined by the principles developed above. In the case of an electron, the spin must adopt a lower-energy state (more or less aligned to the magnetic field) and a higher-energy state (more or less opposed to the magnetic field). The reason of the interaction between an external magnetic field B_0 and a spin, is the existence of magnetic dipole generated by the spinning charged body. The module of the magnetic dipole - represented by the vector μ - is equal to:

$$|\vec{\mu}| = \left(\frac{qh}{4\pi m}\right)\sqrt{I(I+1)} \quad (\text{Eq. II.2})$$

For electrons with $q = -e$, one obtains that μ is then equal to $-g\beta[I(I+1)]^{1/2}$ J.T⁻¹ with a Bohr Magneton β of magnitude $e.h/4\pi m_e = 9.273 \times 10^{-24}$ J.T⁻¹. The electron g-factor is also called the Landé factor, and is equal to 2.00232. For nuclei, on the other hand, the nuclear magnetic moment is equal to $g\beta_N[I(I+1)]^{1/2}$ J.T⁻¹ with a nuclear magneton $\beta_N = eh/4\pi m_p$ of 5.050×10^{-27} J.T⁻¹. Here g is usually called the nuclear g-factor. One can now derive from Eq. II.2 the magnetic dipole of the spin in the z-direction. For electrons, this gives $\mu_z = -g\beta I_z$, while for nuclei μ_z is equal to $g\beta_N I_z$.

An alternative constant is the gyromagnetic or magnetogyric ratio γ , which is defined as the ratio between the magnetic dipole μ_z and the angular momentum I_z . The following equation can then be written: $\mu_z = \gamma I_z$. The value of γ is thus g multiplied with β . Both g and γ are experimental parameters, and the γ -values of the first-row transition metals and a free electron are given in Table II.3. The value of γ can be positive or negative. Negative values implicate that the magnetic moment vectors are opposite in sign to their angular momentum vectors. This is the case for

an electron and for some transition metals, such as ^{53}Cr , and is schematically shown in Figure II.1. It is also clear from Table II.3 that the gyromagnetic ratio γ is much larger for a free electron than for a nucleus. This implies that the magnetic moment of an electron is much larger than that of a nuclear spin, and as a consequence, the sensitivity of ESR spectroscopy is at least three orders of magnitude higher than that of NMR spectroscopy.

The extent of interaction between the magnetic dipole μ_z and the magnetic field B_z applied along the z-axis is equal to the product of the two:

$$\text{Interaction} = \mu_z \cdot B_z \quad (\text{Eq. II.3})$$

The result is that the $2I + 1$ spin states are splitted in energy, with an energy difference equal to:

$$\Delta E = [E_{m_I} - E_{(m_I-1)}] = g\beta m_z B_z - g\beta (m_z-1)B_z = g\beta B_z \quad (\text{Eq. II.4})$$

This is illustrated in Figure II.3 for a spin system with $I = 1/2$, and this splitting forms the basis for spin resonance spectroscopy: a transition of electron or nuclear spins between energy levels, which is associated with the emission or absorption of energy in the form of electromagnetic radiation.

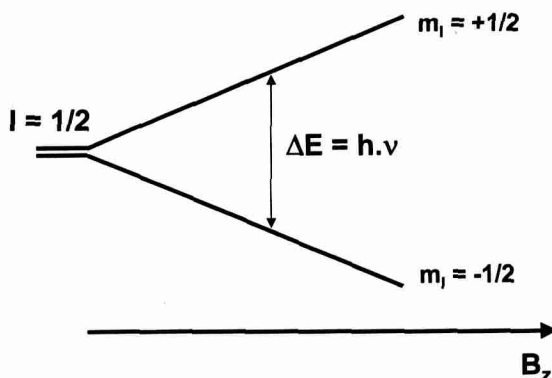


Figure II.3. Splitting diagram for a spin system with $I = 1/2$.

Indeed, the energy difference ΔE corresponds to a particular electromagnetic frequency, since, by the Bohr relation, $\Delta E = h\nu$ with h , the Planck's constant and ν , the radio or microwave frequency (Hz). To take a specific example, if the external magnetic field is 2.35 T, then the energy gap for a free electron is approximately $4.366 \cdot 10^{-23}$ J, and the corresponding resonance frequency is 65.86 GHz, which lies in the microwave band of the electromagnetic spectrum. The resonance frequency for the first-row transition metals at $B = 2.35$ T is given in Table II.3. One can notice that all these frequencies are radiofrequencies.

It is also important to understand what the origin is of the resonance frequencies. Therefore, it is necessary to return to the concept of spinning electron or nucleus. The magnetic field of strength B_z supplies a torque to the spinning charged particle,

causing its magnetic moment to precess. The angular frequency, ω , in radians per second, of this precession – denoted as the Larmor precession – is related to B_z by:

$$\omega = \frac{\mu B_z}{2\pi I} = \frac{g}{h} \beta_N B_z \quad (\text{Eq. II.5})$$

One can calculate then that the Larmor precession occurs with the same frequency as that what is used to excite an electron or nuclear spin from its lowest to its highest energy level. In other words, the spin system comes in resonance.

Finally, we have to introduce the concepts of population of energy levels and the associated relaxation phenomena. Because of thermal motion and the Boltzmann distribution, not all nuclear and electron spins occupy the lowest available energy state. Indeed, classical theory states that at temperature T (K) the ratio of the populations of the energy levels is given by Boltzmann law:

$$\frac{N_{upper}}{N_{lower}} = \exp\left(-\frac{\Delta E}{kT}\right) \quad (\text{Eq. II.6})$$

where, k is the Boltzmann constant. Thus at all temperatures above absolute zero the upper level will always be populated to some extent. One can now calculate for electrons that this population ratio at room temperature is equal to $1 - (1.10^{-3})$, and as a consequence both levels are almost equally populated. Net absorption of electromagnetic radiation in the radio or microwave region by a sample will then only occurs as long as there exists at thermal equilibrium an excess of spin states in the lower energy state. At the moment the population between the two energy states are equal, there will be no further net absorption of radio or microwave frequency energy and the system is said to be saturated. The practical consequence of this saturation is that the ESR or NMR absorption signal will no longer be observable. This net absorption can only be restored if the spins relax. There are two different relaxation processes. In the first, the excess spin energy equilibrates with the surroundings (the lattice) by spin-lattice relaxation having a characteristic spin-lattice relaxation time T_1 . Such relaxation comes about by lattice motions, such as atomic vibrations in a solid lattice and molecular tumbling in liquids and gases. Secondly, there is a sharing of excess spin energy directly between spins *via* spin-spin relaxation, the symbol for the time of which is T_2 .

2.1.3. Electron spin resonance spectroscopy

As was already pointed out before, ESR spectroscopy is a very powerful and sensitive method for the study of TMI with unpaired electrons in their d-shell. There is nowadays a wide variety of ESR techniques available, each with their own advantages and limitations. In continuous wave ESR (CW-ESR), the sample is subjected to a continuous beam of microwave irradiation of fixed frequency and the magnetic field is swept. Different microwave frequencies may be used, which are

denoted as L-band (1.0 GHz), S-band (3.5 GHz), X-band (9.25 GHz), K-band (20 GHz), Q-band (35 GHz) and W-band (95 GHz). All these frequencies are commercially available and can be used as standard tools for spectroscopists, although the commercial W-band instrument only recently became available. The classical set-up is equipped with a klystron diode providing microwaves in X-band, while ESR spectroscopy in W-band (and higher) is called high-frequency ESR. An overview of the different microwave frequencies available is given in Figure II.4. Thus, the preferred experimental set-up is a resonant cavity with coherent microwave sources. One can notice that there is in the scientific community a continuing interest to push the frequency limits to higher values, and at this moment, there are several research projects running on building 300 GHz ESR instruments. However, it is clear that such developments require special instrumental set-ups, and the classical resonance cavities and microwave sources cannot be used anymore. The application of CW-ESR to TMI on surfaces, and their strength and weakness are given in subchapters 2.2 and 2.3.

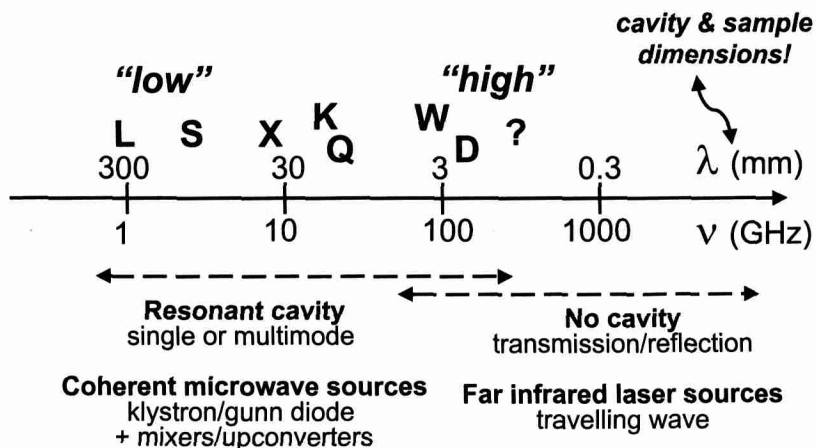


Figure II.4. Different microwave frequencies used in ESR, and its implications towards the design of the spectrometer.

Other techniques, such as electron nuclear double resonance (ENDOR) and electron spin echo envelope modulation (ESEEM) spectroscopies, record in essence the NMR spectra of paramagnetic species, and have proven to be very powerful for elucidating the first and second coordination environment of TMI. ESEEM monitors the spontaneous generation of microwave energy as a function of the timing of a specific excitation scheme; *i.e.*, two or more short resonant microwave pulses, and delivers information about the properties of neighbouring atoms and molecules at rather large distances. ENDOR, on the other hand, detects strongly coupled nuclei surrounding the transition metal ion. Both pulsed ESR techniques require the use of advanced

instrumental equipment. Goldfarb will introduce in subchapter 2.4 the principles, instrumental details and application of ENDOR and ESEEM.

In the next sections, some theoretical and practical aspects of the use of CW-ESR spectroscopy will be treated in order to give the reader sufficient background to understand the different subchapters 2.2-2.4. Emphasis will be placed on the principles of the techniques, the instrumental requirements, spectrum simulation and quantitative analysis.

2.1.3.1. Magnetic interactions

Up to now, we have developed the principles of ESR spectroscopy by considering the hypothetical case of a single isolated electron. It has been shown that the discrete orientations of the angular momentum and magnetic moment vectors were determined by the spin quantum number I , although mostly S is used instead of I for electrons. Thus, a single isolated electron is characterized by the quantum number $S = 1/2$ and possesses a magnetic moment:

$$\vec{\mu}_e = -g_e \beta_e \vec{S} \quad (\text{Eq. II. 7})$$

with g_e , the electron g-factor or Landé-factor, β_e , the electronic Bohr magneton and \vec{S} , the dimensionless electron spin angular momentum vector. In a magnetic field, B_z or B_0 , there are two energy states for this electron, as illustrated in Figure II.5. This interaction, generally known as the Zeeman interaction, is expressed by the following Hamiltonian:

$$H_{Zl} = -\vec{\mu}_e \cdot \vec{B} = g_e \beta_e B_0 S_z \quad (\text{Eq. II. 8})$$

Two energy levels evolve $E_\beta = -1/2 g_e \beta_e B_0$ and $E_\alpha = +1/2 g_e \beta_e B_0$. In ESR, the magnetic component of a microwave energy, which is perpendicular to the magnetic field B_0 , induces microwave energy absorption subject to the resonance condition (Eq. II. 9) and the selection rule $\Delta m_s = \pm 1$:

$$\Delta E = h\nu = g_e \beta_e B_0 \quad (\text{Eq. II. 9})$$

where ν is the microwave frequency (GHz).

In real chemical systems, however, the single unpaired electron is associated with at least one atom and the second contribution to paramagnetism stems from the electron motion in an orbital with orbital angular momentum L . This effect can be described with the following Hamiltonian:

$$H = \beta_e \vec{B} \cdot (\vec{L} + g_e \vec{S}) + \lambda \vec{L} \cdot \vec{S} = \beta_e \vec{B} \cdot \vec{g} \vec{S} \quad (\text{Eq. II. 10})$$

with λ , the spin-orbit coupling constant and g , the effective g -value. The orbitals (atomic or molecular) have two effects: (1) spin-orbit coupling and (2) orbital-magnetic field interaction. These effects explain why g is no longer equal to 2.0023 ($= g_e$) and anisotropic. The anisotropy of the g -tensor leads to orientation-dependent ESR-spectra for single crystals, but for disordered systems as in the case of heterogeneous catalysts, one observes the superposition of spectra of all possible orientations of the magnetic field (powder spectra). Idealized ESR spectra, together with their corresponding absorption profile, are given in Figure II.6. The anisotropy in g is classified into isotropic (one g -value), axial (two g -values) and rhombic (three g -values). The deviation of the principal g -values from the free electron value of 2.0023 carries information about the orbital angular momentum of the electron; *i.e.*, information concerning the electronic structure of the atom or molecules.

The magnetic moment of the electron will also undergo additional interactions with local magnetic fields originating from non-zero nuclear spins. This coupling, known as the hyperfine interaction, is given by:

$$H_{HF} = \bar{I} \cdot \mathbf{A} \cdot \bar{S} \quad (\text{Eq. II.11})$$

with \mathbf{A} the hyperfine coupling tensor, characterized by three mutually orthogonal principal values A_{xx} , A_{yy} and A_{zz} . The point symmetry of the paramagnetic entity determines whether or not any of the principal axes of g and \mathbf{A} are parallel to each other.

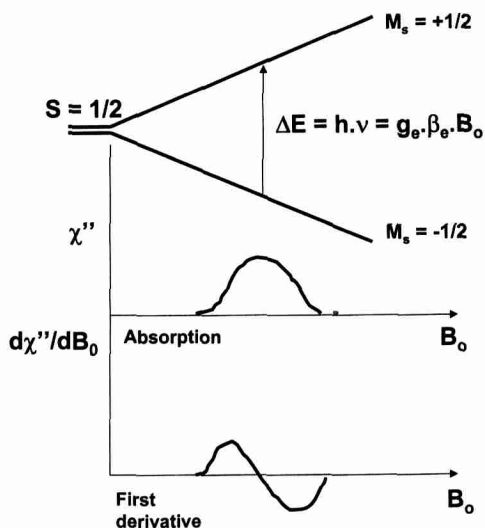


Figure II.5. Energy level diagram for an isolated electron ($S = 1/2$) in a magnetic field B_0 and the corresponding absorption spectrum and first derivative ESR spectrum.

The different possibilities and the relation with symmetry are summarized in Table II.4, together with the generally accepted nomenclature for ESR behavior. The magnetic moment of the electron may also undergo interactions with the local magnetic fields originating from non-zero nuclear spins of atoms in the first coordination sphere around an atom with unpaired electron. This interaction, called superhyperfine splitting, is mostly weak and unresolved.

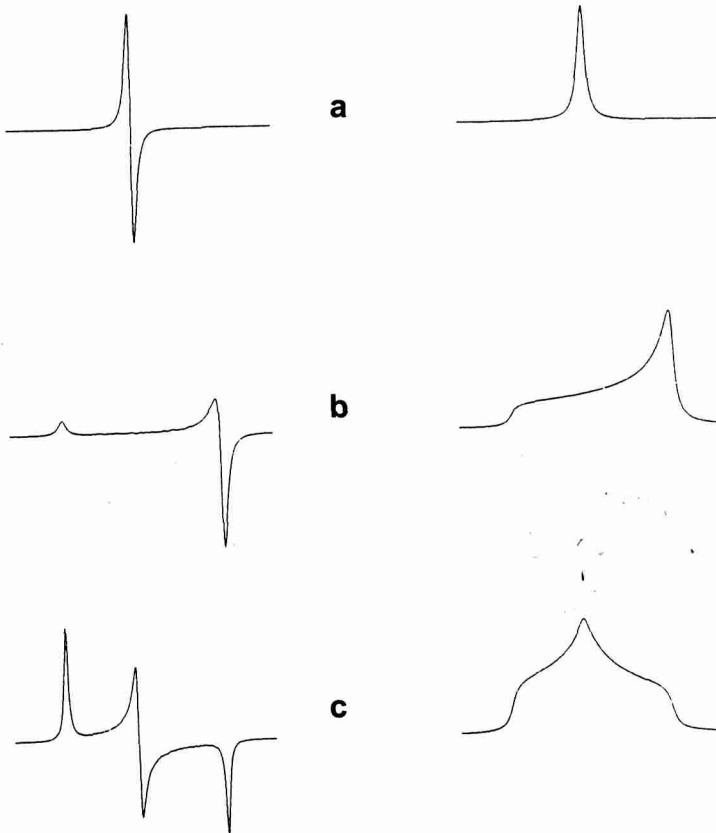


Figure II.6. Idealized powder ESR spectra, together with their corresponding absorption profile: (a) isotropic; (b) axial; and (c) rhombic.

Some nuclei with nuclear spins $I \neq 1$ possess an electric quadrupole moment eQ because of the non-spherical charge distribution in the nucleus. The interaction with such nuclei is the quadrupole interaction:

$$H_q = \bar{I} \cdot \mathbf{Q} \cdot \bar{I} \quad (\text{Eq. II.12})$$

with \mathbf{Q} the quadrupole coupling tensor. As in the case of the magnetic moment of the electron, also the magnetic moment of the nucleus interacts with the magnetic field \vec{B} . This causes a further term in the spin Hamiltonian:

$$H_{NZ} = -g_N \beta_N \vec{B} \cdot \vec{I} \quad (\text{Eq. II.13})$$

with β_N the nuclear magneton and g_N the nuclear g-factor, which is characteristic for each isotope. Usually this term is negligible in regular ESR, but important in ENDOR spectroscopy.

If two or more unpaired electrons are present, so that the total spin S of the electron system is greater than $1/2$, one has to take into account the interaction of the electrons with the electric field generated by the surrounding atoms (*i.e.*, the crystal field or ligand field). This interaction causes a splitting of the more than twofold (Kramers-) degenerated ground state of the electron system even in the absence of an external magnetic field (*i.e.*, zero field splitting). This results in a line splitting in the ESR spectrum and this interaction can be described by the following Hamiltonian:

$$H_{FS} = \vec{S} \cdot \mathbf{D} \cdot \vec{S} \quad (\text{Eq. II.14})$$

with the traceless fine structure tensor \mathbf{D} . The Hamiltonian becomes [9]:

$$H_{FS} = D(\bar{S}_z^2 - \frac{S(S+1)}{3}) + E(\bar{S}_x^2 - \bar{S}_y^2) \quad (\text{Eq. II.15})$$

Here D denotes the axial fine structure parameter, whereas E describes the orthorhombic fine structure parameter [9].

Table II.4. Relationships between \mathbf{g} and \mathbf{A} tensors, ESR symmetry and the point symmetry of paramagnets.

ESR symmetry	\mathbf{g} and \mathbf{A} tensors	Coincidence of tensor axes	Molecular point symmetry
Isotropic	$g_{xx}=g_{yy}=g_{zz}$ $A_{xx}=A_{yy}=A_{zz}$	all coincident	O_h, T_d, O, T_h, T
Axial	$g_{xx}=g_{yy} \neq g_{zz}$ $A_{xx}=A_{yy} \neq A_{zz}$	all coincident	$D_{4h}, C_{4v}, D_4, D_{2d}, D_{6h}, C_{6v}, D_6, D_{3h}, D_{3d}, C_{3v}, D_3$
Rhombic	$g_{xx} \neq g_{yy} \neq g_{zz}$ $A_{xx} \neq A_{yy} \neq A_{zz}$	all coincident	D_{2h}, C_{2v}, D_2
Monoclinic	$g_{xx} \neq g_{yy} \neq g_{zz}$ $A_{xx} \neq A_{yy} \neq A_{zz}$	one axis of \mathbf{g} and \mathbf{A} coincident	C_{2h}, C_s, C_2
Triclinic	$g_{xx} \neq g_{yy} \neq g_{zz}$ $A_{xx} \neq A_{yy} \neq A_{zz}$	complete non-coincidence	C_1, C_i
Axial non-collinear	$g_{xx} \neq g_{yy} \neq g_{zz}$ $A_{xx} \neq A_{yy} \neq A_{zz}$	only g_{zz} and A_{zz} coincident	$C_3, S_6, C_4, S_4, C_{4h}, C_6, C_{3h}, C_{6h}$

Summarizing, four different magnetic interactions may occur, which influence the behavior of electrons in a magnetic field: (a) the Zeeman interaction, H_{ZI} ; (b) the nuclear hyperfine interaction, H_{HF} ; (c) the electrostatic quadrupole interaction, H_Q and (d) the zero-field splitting if $S > 1/2$, H_{FS} . The sum of these interactions results in the total spin Hamiltonian, H_T :

$$H_T = \beta_e \bar{B} \cdot \mathbf{g} \cdot \bar{S} + \bar{I} \cdot \mathbf{A} \cdot \bar{S} + \bar{I} \cdot \mathbf{Q} \cdot \bar{I} + \bar{S} \cdot \mathbf{D} \cdot \bar{S} \quad (Eq. II.16)$$

2.1.3.2. Instrumentation

The basic components of a classical low-frequency ESR spectrometer are shown in Figure II.7 [17]. The microwave bridge supplies microwaves at a fixed frequency and chosen power, and the microwave source is a klystron or a gundiode. The most commonly used frequency is *ca.* 9.25 GHz (X-band) and the corresponding resonance field for $g = 2$ is 0.3300 T. Q-band ESR, at *ca.* 35 GHz, is the next commonly used frequency, which gives transitions at 1.2500 T for $g = 2.0$. The microwaves are transmitted to a sample cavity *via* a waveguide. The sample cavity is a device in which the sample can be irradiated with the microwave energy, but which is also capable of being tuned so that microwave energy can be reflected back to a detector in the microwave bridge.

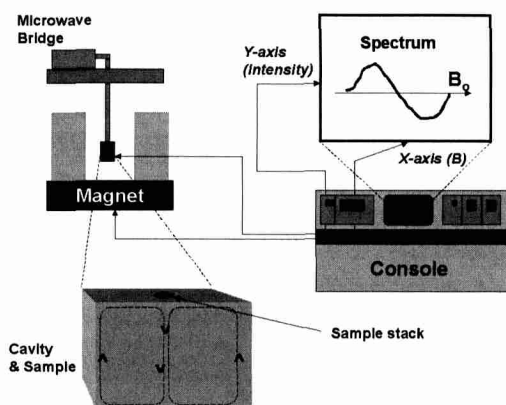


Figure II.7. General layout of a classical low-frequency ESR spectrometer.

The design of the cavity depends mainly on the applied microwave frequency because the dimensions of the cavity (and waveguide) must match the wavelength of the microwaves. The wavelength (and cavity dimensions) for X- and Q-band are 3.24 and 0.86 cm, respectively. It is also clear that these size limitations have a strong influence on the maximum amount of sample that a particular cavity will tolerate. For example, Q-band cavities permit only the use of very small amounts of samples, and the use of high-frequency techniques put even more severe limitations on the cavity and sample

dimensions (Figure II.4). The sample cavity is then placed perpendicular to the applied magnetic field, B_0 , which can be varied in a controlled way. B_0 is generated by an electromagnet and should be as accurate and homogeneous as possible. In addition to the main magnetic field a controlled but smaller oscillating magnetic field is superimposed on the sample cavity *via* the modulation coils. Thus, the signal response from the cavity is modulated at the modulation frequency, and this results in a first derivative ESR spectrum. The ideal way to perform an ESR experiment would be to apply a fixed magnetic field and to vary the microwave frequency. However, microwave sources are tunable only over limited ranges. Therefore, the microwave frequency is kept constant and the applied magnetic field is varied over a field range wherein microwave absorption is expected. This is called continuous wave electron spin resonance (CW-ESR). At this stage, the intensity change of the reflected microwave energy is measured by the detector and the obtained signal is amplified, recorded and stored for further treatment.

The following parameters must be optimized to obtain a physically meaningful ESR spectrum:

(i) *magnetic field scan range*: If one does not know much about a sample, it is advisable to scan the widest magnetic field range available. Afterwards, one may pick up the scan range of interest.

(ii) *modulation amplitude*: An oscillating magnetic field at a fixed and stable frequency (mostly 100 kHz) is applied to the sample cavity *via* coils. The magnetic field is applied continuously throughout the experiment. The amplitude of this modulation is very important because too high modulation amplitudes may distort the individual lines in a spectrum so that valuable information is lost. This is especially important when the lines are sharp and weak.

(iii) *sweep time*: Short sweep times may significantly distort the ESR spectrum in that (a) the cross-over point of the first derivative spectrum may be shifted in the direction of the scan; (b) the spectrum becomes asymmetric or (c) the signal intensity reduces.

(iv) *sample temperature*: Low concentrations of paramagnetic entities may become only visible at low measuring temperature. Furthermore, measurements of the signal intensity as a function of the sample temperature allow to distinguish different types of magnetic behavior (*i.e.*, paramagnetism, anti-ferromagnetism, etc.);

(v) *microwave power*: At low values of the microwave power the signal amplitude will increase in direct proportion to the square root of the microwave power received by the sample. This relationship, however, is only obeyed up to a certain power level, beyond which the signal intensity levels off or even decreases. This is known as microwave power saturation and no quantitative information can be extracted from saturated spectra. Saturation effects are also more pronounced at low temperatures.

If one wants to determine g -values from ESR spectra, one has to know both the field B_0 and the microwave frequency ν (Eq.II.9). There are two possible methods: One can use a Gaussmeter and a frequency counter, both of which are relatively expensive instruments; the second method is based on the use of a standard with accurately known g -values. A double rectangular cavity (TE_{104}) is very convenient in that the standard

(REF) is placed in one half of the cavity and the (unknown) sample (M) in the other. Only one cavity tuning operation is necessary for both measurements. With DPPH (diphenylpicrylhydrazine) as standard with $g_{REF} = 2.0036$, one has:

$$h\nu_{REF} = g_{REF}\beta B_{0,REF} \quad (Eq. II.17)$$

$$h\nu_M = g_{eff}\beta B_{0,M} \quad (Eq. II.18)$$

with: $h\nu_{REF} = h\nu_M$ or $g_{eff} = g_{REF}(B_{0,REF}/B_{0,M})$ (Eq. II.19)

The resonance fields $B_{0,REF}$ and $B_{0,M}$ are read directly from the ESR spectra.

2.1.3.3. Quantitative analysis

The concentration, C , of a paramagnetic entity in a sample, subjected to an ESR experiment, is given by Eq. II.20 [9]:

$$C = \frac{KI}{GP} \quad (Eq. II.20)$$

with K , a proportionality constant; I , the ESR line intensity; G , the amplifier gain of the spectrometer and P , the ESR transition probability [9]. The proportionality constant K is dependent on (a) the properties of the sample cavity, (b) the applied microwave power and (c) the applied modulation amplitude. The intensity I of the ESR signal must be obtained by working in the linear region of the microwave detectors and in the absence of microwave power saturation (*i.e.*, low paramagnetic concentrations). It is important to stress that an ESR signal consists of the first derivative of the absorption line and the ESR intensity must be related with the area under the absorption envelope. This is done by double integration of the recorded first derivative spectrum over a well-defined scan range.

If the number of spins in a standard is accurately known, its signal intensity can be used to determine the number of spins in the unknown sample. It is clear that K and P of Eq. II.20 must be identical for the standard and the (unknown) sample. The related implications are that conditions (a) to (c) should be identical for the paramagnetic sample and for the standard. Condition (a) means that the sample container, the volume of sample, the positioning in the sample cavity and the dielectric properties of both samples are identical. In addition, the standard should ideally have ESR properties (electronic structure, g -values, etc.) identical to those of the studied paramagnetic entity. Because this is almost impossible, one should choose a standard which is as close as possible to that of the unknown.

If the spectra of the paramagnetic entity in the unknown sample (M) and of the standard or reference compound (REF) have the same number of features spread over the same magnetic field range and if these spectra are integrated over the same scan range, then ESR allows the quantification of this paramagnetic entity according to Eq. II.21:

$$N_M = N_{REF} \left(\frac{A_M}{A_{REF}} \right) \left(\frac{g_{REF}}{g_M} \right) \left(\frac{S_{REF}(S_{REF}+1)}{S_M(S_M+1)} \right) \text{ (Eq. II.21)}$$

with: N_M , N_{REF} = amount of spins of M and reference compound, respectively; A_M , A_{REF} = intensity of the ESR signal of M and reference compound obtained after double integration, respectively; g_M , g_{REF} = g-value of M and reference compound, respectively and S_M , S_{REF} = spin quantum number of M and reference compound, respectively. The last term in Eq. II.21 corrects for the differences between the spin quantum number of the unknown and that of the reference compound.

Double integration of the ESR signal is not straightforward, especially in the case of TMI with their spectra smeared out over a broad magnetic field range. The following parameters must be known or chosen:

- (i) *lineshape*: This can be either Gaussian, Lorentzian or a combination of both;
- (ii) *baseline*: Integration is always very sensitive to baseline effects. A constant offset, for example, which means that the whole spectrum is shifted up or down from zero, results in a quadratic baseline in the doubly integrated spectrum. If integration is carried out over a wide range, such effect becomes large. This can be corrected by choosing a suitable baseline correction (cubic, linear, etc.).
- (iii) *integration width*: Each spectrum must be integrated over the same scan range so that the same number of features are taken into account. Furthermore, large integration widths are recommended because tailing effects may cause important contributions to the overall spectrum.

It is clear that a quantitative determination of paramagnetic species is rather complicated and requires a great deal of experimental care. Therefore, absolute determination of paramagnetic entities, especially transition metal ions, can only be done within 10 to 20 % accuracy and explains why the number of quantitative ESR studies in the field of heterogeneous catalysis is limited.

2.1.3.4. Spectrum simulation

For the simulation of the ESR spectra one has to solve the spin Hamiltonian of Eq. II.16. The easiest way to do this is to regard all the different terms in the spin Hamiltonian as small compared with the electron Zeeman interaction and to use perturbation theory of the first order. The Zeeman term can easily be solved within the eigensystem of the S_Z operator (in the main axis system of the g-tensor or $\vec{S}_{Zl} = \vec{B}$ for isotropic cases), for instance in the isotropic case:

$$E^{Zl} = g\beta B m_s \text{ (Eq. II.22)}$$

Unfortunately, in most cases this simplification is not applicable. Therefore, the use of perturbation theory of higher order is recommended, or in more complicated

situations, the diagonalization of the spin Hamiltonian within the eigensystem of its spin operators.

Because the ESR experiment does not measure the energy spectrum for one fixed magnetic field by scanning the frequency of the microwave, but scans the magnetic field, it is necessary to calculate the energy levels for each magnitude of the magnetic field and to determine the resonance fields by comparing the differences of the energy levels with the applied microwave energy. Therefore, the spin Hamiltonian needs to be diagonalized very often and such calculations are time consuming. For the calculated resonance positions it is easy to determine the appropriate intensities by evaluating the transition probabilities which can be calculated using the eigenfunctions of the spin Hamiltonian.

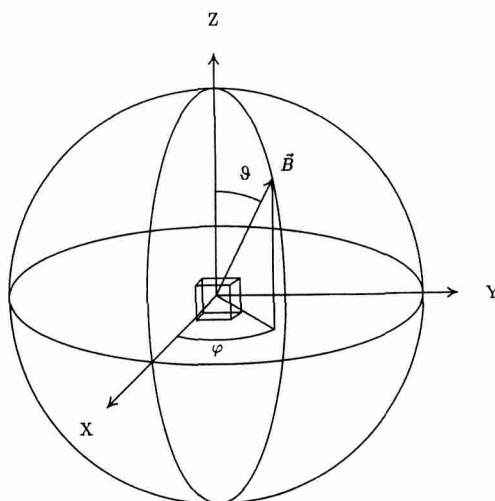


Figure II.8. Definition of the polar angles of the applied magnetic field, B_0 , with their respect to the principal axes.

For powdered samples, the contributions of all possible orientations of the magnetic field have to be taken into account. This is illustrated in Figure II.8. Thus, the above described calculations need to be summed up for all orientations (*i.e.*, integration about φ in the axial case and about φ and θ in orthorhombic systems). Eventually the line shape has to be taken into account by convolution of the result with the appropriate line shape function (*e.g.*, Gaussian or Lorentzian line with a suitable line width). There are a lot of simulation programs available in literature, either based on perturbation or matrix diagonalization methods : MAGRES (from the Department of Molecular Spectroscopy in Nijmegen, The Netherlands); MSPEN/MSGRA (from the group of Hütterman in Hamburg, Germany); QPOW (from the group of Belford, University of Illinois, USA); EPR.FOR (from the group of Weil, University of Saskatchewan, Canada), Manchester program (from the group of Mabbs and Collison, Manchester University, UK) and Pilbrow program (from the

group of Pilbrow, Monash University, Australia). Details about these programs can be found in the textbook of Mabbs and Collison [9].

In practice, one usually wishes to determine accurately the parameters of the spin Hamiltonian out of the measured spectrum. Therefore one has to estimate the parameters (g , D , E , A , Q , the line shape and the line width) to simulate the spectrum and to compare the result with the experimental spectrum, eventually followed by re-estimation of the parameters and simulation.

2.1.4. References

- [1] C.P. Schlichter, Principles of magnetic resonance, with examples from solid state physics, Harper & Row, New York, Evanston and London, 1963.
- [2] A. Carrington and A.D. McLachlan, Introduction to magnetic resonance, with applications to chemistry and chemical physics, Harper & Row, New York, Evanston and London, 1967.
- [3] W. Kemp, NMR in chemistry, a multinuclear introduction, Macmillan Education Ltd., London, 1986.
- [4] C.N. Banwell, Fundamentals of Molecular Spectroscopy, 3rd Ed., McGraw-Hill, London, 1983.
- [5] A. Abragam and B. Bleaney, Electron paramagnetic resonance of transition metal ions, Clarendon Press, Oxford, 1970.
- [6] J.R. Pilbrow, Transition Ion Electron Paramagnetic Resonance, Clarendon Press, Oxford, 1990.
- [7] N.M. Atherton, Electron spin resonance, theory and applications, Ellis Horwood Ltd, Chichester, 1973
- [8] J.E. Wertz and J.R. Bolton, Electron spin resonance, elementary theory and practical applications, Chapman and Hall, New York, 1986.
- [9] F.E. Mabbs and D. Collison, Electron Paramagnetic Resonance of Transition Metal Compounds, Elsevier, Amsterdam, 1992.
- [10] C.P. Poole, Electron spin resonance: a comprehensive treatise on experimental techniques, Interscience Publishers, a division of John Wiley and Sons Inc, New York, 1976.
- [11] T.H. Wilmshurst, Electron spin resonance spectrometers, Hilger, London, 1967.
- [12] R.S. Alger, Electron paramagnetic resonance techniques and applications, Interscience Publishers, a division of John Wiley and Sons Inc, New York, 1986.
- [13] J.S. Hyde and W. Froncisz, Specialist Periodical Reports: Electron Spin Resonance, Royal Society of Chemistry, Vol 10, 1981.
- [14] J.C. Vedrine, Characterization of Heterogeneous Catalysts, F. Delannay (Ed.), Marcel Dekker, New York, 1984, p. 161.
- [15] F.E. Mabbs, Chem. Soc. Rev., 1993, 314.
- [16] J.H. Lunsford, Adv. Catal., 1972, 22, 265.

- [17] R.T. Weber, ESP 300 E ESR Spectrometer User's Manual, Bruker Instruments, Inc, Billerica, Massachusetts, USA, 1992.
- [18] A. Schweiger, *Angew. Chem.*, 1991, 103, 223.
- [19] W.B. Mims, in *Electron Paramagnetic Resonance*, Geschwind S (Ed), Plenum Press, New York, 1992, 263.
- [20] M. Heming, *Z. Phys. Chem. Neue Folge*, 1987, 151, 35.
- [21] M. Mehring, *Z. Phys. Chem. Neue Folge*, 1987, 151, 1.
- [22] G. Martini, *Colloids and Surfaces*, 1990, 45, 83.
- [23] L. Kevan and M.K. Bowman, *Modern Pulsed and Continuous Wave Electron Spin Resonance*, Wiley, New York, 1990.
- [24] R.A. Drago, *Physical Methods in Chemistry*, E.B. Saunders Company, Philadelphia, 1997.